Dependence of NO_2 sensitivity on thickness of oxide-sensing electrodes for mixed-potential-type sensor using stabilized zirconia

Perumal Elumalai · Vladimir V. Plashnitsa ·
Taro Ueda · Masaharu Hasei · Norio Miura

Abstract The effect of thickness of oxide-sensing electrode (SE) on NO_2 sensitivity of the planar sensor based on yttria-stabilized zirconia (YSZ) was examined at high temperatures. The sensitivity of the sensor increased with decreasing thickness of SE, and the highest sensitivity was obtained by using the thinnest layer of Cr_2O_3–SE (2.7 μm) at 700 °C. In the case of NiO–SE, the highest sensitivity was observed for the sensor using the 4-μm-thick SE even at a high temperature of 850 °C. Based on the results of the measurements for the complex impedances, the polarization curves, and the gas-phase NO_2 decomposition catalysis, it was confirmed that the catalytic activity to the gas-phase NO_2 decomposition on the oxide–SE matrix played an important role in determining the NO_2 sensitivity of the present sensors.

Keywords NOx sensor · Mixed potential · YSZ · NiO · Cr_2O_3

P. Elumalai · V. V. Plashnitsa · N. Miura (✉)
Art, Science and Technology Center for Cooperative Research,
Kyushu University,
Kasuga-shi,
Fukuoka 816-8580, Japan
e-mail: miura@astec.kyushu-u.ac.jp

T. Ueda
Interdisciplinary Graduate School of Engineering Sciences,
Kyushu University,
Kasuga-shi,
Fukuoka 816-8580, Japan

M. Hasei
R&D Division, Riken Corporation,
Kumagaya-shi,
Saitama 360-8522, Japan

Introduction

Nitrogen oxides (mainly NO and NO_2, referred as NOx) are formed in any combustion process, especially in automotive engines. Among the main environmental air pollutants, nitrogen oxides are of the greatest concern, as they are directly related to vehicle exhausts. They transform to gaseous nitric acid and toxic organic nitrates in air atmosphere, and hence result in the production of acid rain, photochemical smog, and the like in the environmental ecosystem. Consequently, in view of the higher strict regulation of emissions from automobiles, the need for a new generation of in situ, cost-effective, and reliable gas sensors has become a high priority [1, 2]. Such sensors must be able to provide a stable and unambiguous signal in harsh environments at elevated temperatures. To satisfy the recent automobile emission regulations, the on-board diagnosis (OBD) system has been proposed to be used inside vehicles to monitor all the gaseous components related to air pollution.

In this OBD system, two oxygen sensors (lambda sensors) can be used: one placed upstream of the conventional three-way catalyst (TWC) to control the air/fuel ratio and the second one located downstream in the exhaust to control the efficiency of the catalytic converter. Due to the fact that the NOx removal efficiency of the TWC is significantly low under lean region (air rich), a new NOx-storage catalyst needs to be used in addition to the conventional oxygen sensors. In this regard, to monitor the regenerate time and NOx concentration in the exhausts, it is highly desired to develop high-performance NOx sensors. Such a new and reliable solid-state NOx sensor will allow direct and precise analysis of the pollutants, easily integrable in the OBD system of direct-injection-type gasoline engines operating in lean region.

So far, mixed-potential-type sensors based on YSZ and oxide–SEs are considered to be good candidates in regard to their special features such as compactness, fast response, and low cost [3–20]. However, the sensitivity is considerably low, especially at temperatures in excess of 700 °C. Quite recently, our group has reported that the YSZ-based sensor using NiO–SE could be operated with high NO_2 sensitivity even at temperatures higher than 800 °C under humid condition [21–25]. Addition of noble metal (Rh) to NiO–SE improved the performances of the sensor [25]. As far as the requirements of automotive NOx sensors are concerned, working temperature of sensor at or above 800 °C is an important issue, due to the fact that the temperature of a car engine sometimes reaches up to even 900 °C during acceleration of vehicles [22–24].

The NO_2 sensitivity was found to depend on the kind of SE, morphology of SE, and sintering temperature of SE [22, 23, 26]. Thickness of SE is also one of the important factors for determining NO_2 sensitivity of the mixed-potential-type sensor [27]. So, we examined in this study in more detail the influence of thickness of NiO–SE (or Cr_2O_3–SE) on NO_2 sensitivity and the reason for occurrence of the thickness effect based on the results obtained from the measurements of the difference in potential (emf) responses, complex impedances, polarization curves, and gas-phase catalytic activity. The reason why these two oxides have been chosen is that NiO can be used as an SE for high-temperature operation as mentioned above [21–25] and Cr_2O_3 is now tested as an SE for the prototype laminated-type sensor [28].

Experimental

Fabrication of sensor

The homemade Y_2O_3-added (8 wt%) zirconia plates were used for the fabrication of the planar NO_2 sensor. The physical dimensions of the YSZ plates are 10×10 mm, at 0.2 mm thickness. The schematic cross-sectional view of the planar sensor used in this study is shown in Fig. 1. The Pt
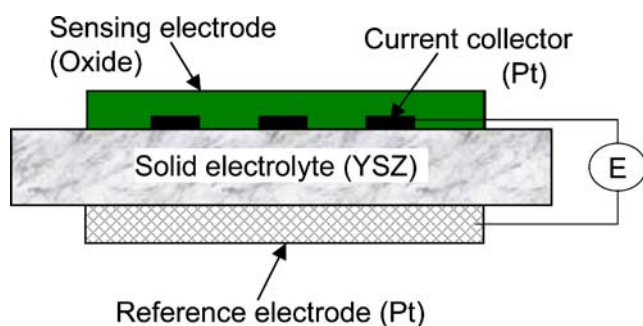

Fig. 1 Schematic cross-sectional view of the planar sensor used

paste was screen-printed on both sides of YSZ plate and annealed at 1,000 °C for 2 h in air. The commercially available NiO (or Cr_2O_3) powder was mixed with α-terpineol and the resulting paste was printed on the transfer paper by means of screen-printing method. The fabrication process of the oxide layer on the front side of the YSZ plate having a Pt-stripe electric collector was done by means of slide-off-printing technique, as described elsewhere [28, 29].

To increase the thickness of the SE layer, the required number of the oxide film was laminated on the YSZ plate. To make a good electrical contact with a measuring equipment, Pt wires (0.1 mm in diameter) were spot-welded by using a Pt paste onto the Pt-connecting spots of each of SE and reference electrode (RE) layers. Finally, the YSZ plate attached with the oxide layer was sintered at 1,400 °C for 2 h in air to form SE.

Characterization of sensing materials

The crystal structures of NiO and Cr_2O_3 were examined by means of an X-ray diffractometer (XRD, RIGAKU, RINT 2100VLR/PC). The CuKα radiation ($\lambda=1.5406$ Å) and 0.5°/min angle step were used for all measurements. The surface morphology and thickness of SE were observed by using a field emission scanning electron microscopy (JEOL, JSM-340F), operating at 15 kV.

Measurements of sensing characteristics

The measurements of sensing characteristics were carried out by using a conventional gas flow apparatus equipped with a furnace operating in the temperature range of 700–900 °C. The 5 vol.% O_2 (+N_2 balance) was used as a base gas. The NO_2 concentration in the sample gas was changed from 50 to 400 ppm. The base gas and the sample gas were humidified with 5 vol.% water vapor by using a water-vapor generator coupled with a small evaporator and a micro-flow pump (Hitachi, L-2100). Both of the base gas and the sample gas were allowed to flow over the sensor at a constant flow rate of 100 cm^3/min. SE and RE were exposed simultaneously to the sample gas or the base gas. The difference in potential between SE and RE of the planar sensor was measured with a digital electrometer (Advantest, R8240) as a sensing signal. The potential of the SE was always positive with respect to RE.

The current–voltage (polarization) curves were measured by means of an automatic polarization system (Hakuto Denko, HZ-3000) based on potential-sweep method at a scan rate of 2 mV/min for a two-electrode configuration in the base gas (5 vol.% O_2 + N_2 balance) and in the sample gas containing 200 ppm NO_2 (+ base gas). The current axis of the anodic polarization curve was subtracted from that of the cathodic polarization curve at

each potential so as to obtain the modified polarization curve in which the current axis was expressed in absolute scale. The complex impedance of the sensor was measured in the frequency range from 0.01 Hz to 1 MHz, with 50 mV exciting voltage by means of an impedance analyzer (Solatron, 1255 WB) at 700 °C (or 850 °C).

Evaluation of catalysis for gas-phase NO$_2$ conversion

The catalytic activity against the gas-phase decomposition of NO$_2$ to NO was evaluated in the temperature range of 200–900 °C for each of NiO–SE (or Cr$_2$O$_3$–SE) layers having different thicknesses, by using a conventional gas flow apparatus as well as a chemiluminescence NOx analyzer (Yanaco, ECL-88A).

Results and discussion

Characterization of SE layer

To examine the thermal stability of NiO and Cr$_2$O$_3$, XRD patterns (not shown here) were recorded for each of the SE layers having different thicknesses sintered at 1,400 °C. It was observed that the NiO–SE and the Cr$_2$O$_3$–SE retain the crystallographic phase corresponding to JCPDS PDF no.: 44-1159 (face-centered cubic) and no.: 38-1479 (Rhombohedral), respectively. This means that NiO and Cr$_2$O$_3$ are quite stable even after sintering at such high temperature. However, all the peaks assigned to both of the oxides were very narrow due to sintering effect.

The representative SEM images of cross-section of NiO–SEs are shown in Fig. 2. It is seen that NiO–SE have different thicknesses of about 4, 7, and 11 μm and the thickness was almost uniform throughout the matrix. Almost the same thickness was also observed in the case of Cr$_2$O$_3$–SE, except for the thinnest layer (2.7 μm). The state of interface (YSZ/NiO or YSZ/Cr$_2$O$_3$) was confirmed to be almost equal irrespective of thickness of oxide layer as shown in Fig. 3. As the state of interface is the same in each case, it is expected that the rate of electrochemical reactions, especially anodic reaction of oxygen and hence recovery rate, should be equal irrespective of the thickness of SE. The surface of each SE layer consisted of almost uniform grains and uniform pores. The average grain size of NiO and Cr$_2$O$_3$ was about 3 and 2 μm, and the average pore size was about 0.7 and 0.5 μm, respectively.

Effect of thickness on NO$_2$ sensitivity

The emf responses to various NO$_2$ concentrations were examined for the sensors using each of different thicknesses of NiO–SE and Cr$_2$O$_3$–SE at 850 and 700 °C, respectively.

Figure 4 shows the representative response transients to 200 ppm NO$_2$ for the sensors using each oxide–SE having various thicknesses. It is seen that the emf value changed quickly from the base level when the sample gas was introduced onto the sensors and the steady-state emf values were attained in due time in each case. The response and recovery rates of the sensors were almost the same, irrespective of the thickness of oxide–SE used. The typical 90% response and recovery times of the sensor using 7-μm-thick NiO–SE at 850 °C were about 12 and 72 s, respectively.

Figure 5 shows the dependence of NO$_2$ sensitivity on the concentration of NO$_2$ at 850 °C for the sensor attached with each NiO–SE having various thicknesses. It is seen that the emf of the sensor varied linearly with NO$_2$ concentration on a logarithmic scale in the examined concentration range. Such a linear variation is typical for the mixed-potential-type sensor, as reported before [2–25].
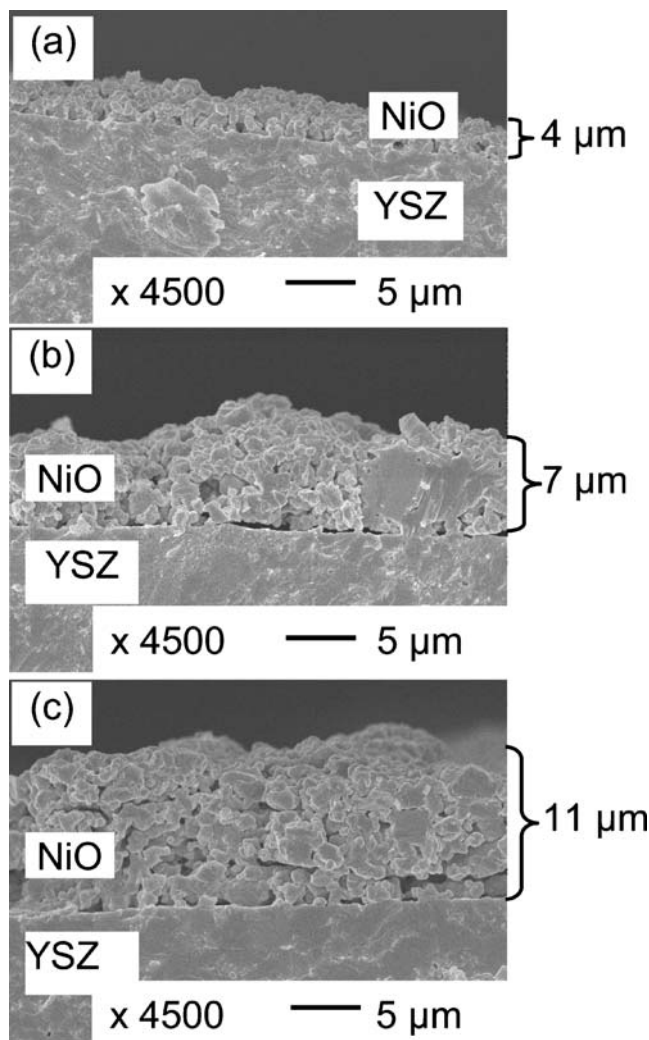

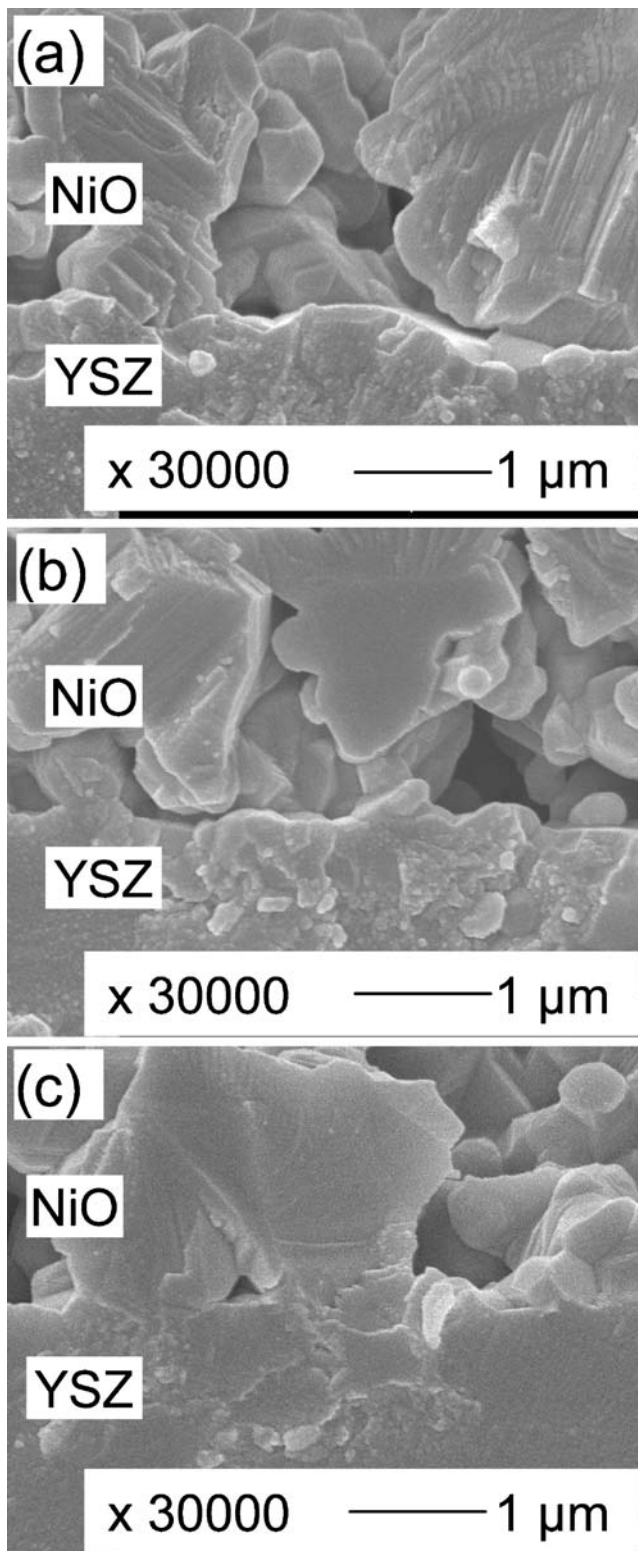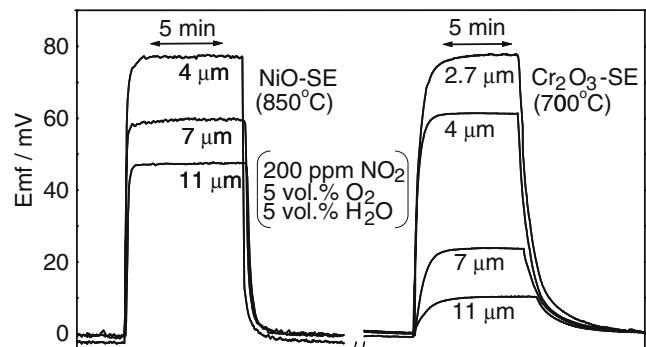**Fig. 2** SEM images of cross-sections of NiO–SEs. SE thickness: **a** 4 μm, **b** 7 μm, and **c** 11 μm

Fig. 4 Response transients to 200 ppm NO_2 for the planar sensors attached with NiO–SE (or Cr_2O_3–SE) having various thicknesses

sensitivity increases with decreasing thickness of SE and the highest sensitivity was obtained for the sensor attached with the thinnest NiO–SE (4 μm). In the case of Cr_2O_3, the highest sensitivity was seen for the sensor using 2.7-μm-thick SE and the emf value was as high as ca. 78 mV even at 700 °C. There is a possibility to obtain still higher sensitivity if the SE thickness is decreased further.

Electrochemical catalytic activity

To rationalize the above-mentioned sensing characteristics, the complex-impedance measurements were performed in the base gas (5 vol.% O_2 + N_2 balance) and in the sample gas containing 400 ppm NO_2 (+ 5 vol.% O_2 + N_2 balance) for the planar sensors using each of NiO–SEs (or Cr_2O_3–SEs) having various thicknesses. The Nyquist plots at 850 °C in the base gas and in the sample gas for the sensor attached with each of various thickness of NiO–SE are shown in Fig. 7, as the representative examples. It is seen that, in each case, the impedance spectrum was in the form
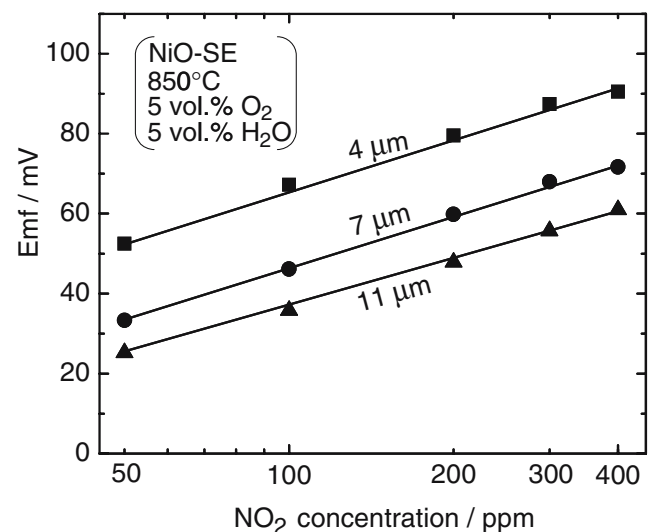

Fig. 3 SEM images of the vicinity of YSZ/NiO interface. SE thickness: **a** 4 μm, **b** 7 μm, and **c** 11 μm

Figure 6 shows the dependence of sensitivity (emf) to 200 ppm NO_2 on the thickness of NiO–SE and Cr_2O_3–SE at 850 and 700 °C, respectively. It is seen that the NO_2

Fig. 5 Variation of NO_2 sensitivity with concentration of NO_2 at 850 °C for the sensor attached with each of various thickness of NiO–SE under wet condition (5 vol.% H_2O)

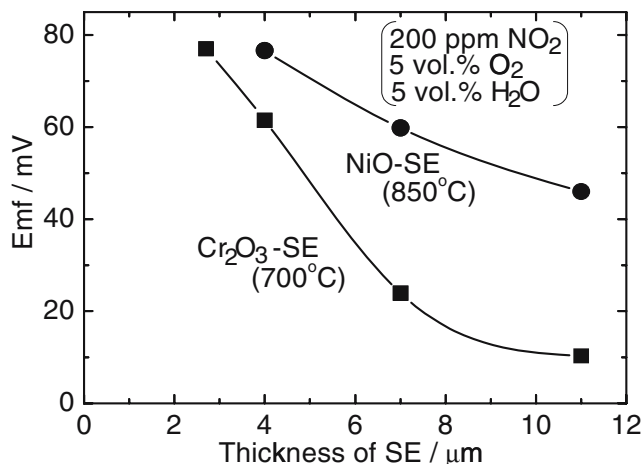Fig. 6 Dependence of NO₂ sensitivity on thickness of NiO–SE (or Cr₂O₃–SE) for the planar zirconia-based sensor
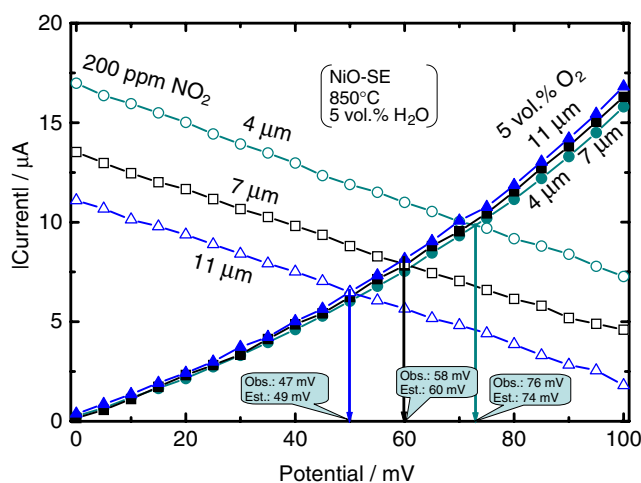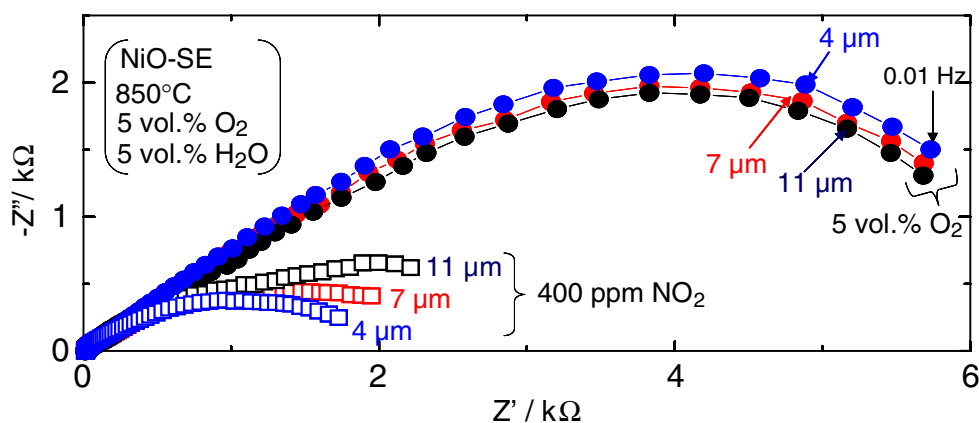

Fig. 8 Modified-polarization curves in 5 vol.% O₂ and in 200 ppm NO₂ for the planar sensor attached with each of various thickness of NiO–SE at 850 °C under wet condition (5 vol.% H₂O)

of a semicircle. In the base gas, the diameter of semicircle, which reflected the resistance of electrode reaction involving O₂ [30–32] was hardly affected by the thickness of oxide–SE. Almost the same results were also observed for the sensor attached with each of various thickness of Cr₂O₃–SE at 700 °C.

This implies that the catalytic activity for the electrochemical reaction of O₂ occurring at the YSZ/oxide interface is almost equal irrespective of the SE thickness. This seems to occur because it was confirmed from the SEM observation that the state of interface where the electrochemical reactions proceed in each case was almost the same irrespective of thickness of SE (Fig. 3). Thus, it is understandable that the sensors exhibit almost equal recovery rates. On the other hand, the diameter of the impedance plots in the sample gas is a bit decreasing with decreasing thickness of SE layer. This seems to indicate that, at the interface of YSZ/oxide, the actual NO₂ concentration is high in the case of thinner SE layer. Unlike in the present case, we have recently reported that the rate of electrochemical reactions and hence the

response/recovery rates was strongly influenced by state of YSZ/oxide interface [21].

When a larger number of reaction site is present at YSZ/oxide interface, the sensor exhibits faster response/recovery rates, while when the number of reaction site is significantly lower, sensor exhibits slower response/recovery rates. Thus, it can be said that if the number of reaction site at interface is equal (for one kind of SE), the sensor should exhibit almost equal response/recovery rates as has been observed in the present case.

To substantiate the impedance results, current–voltage (polarization) curves were measured for the sensor using each of SEs having different thicknesses. Figure 8 shows the modified polarization curves for the sensor using each of various thickness of NiO–SE at 850 °C. It is clearly seen that the anodic polarization curve of O₂ is almost invariant with thickness of SE layer used. Such invariance of anodic polarization curves confirms that the rate of anodic reaction occurring at the interface is almost the same in all thicknesses of SE layer as has been observed from the impedance results. In contrast, the cathodic polarization
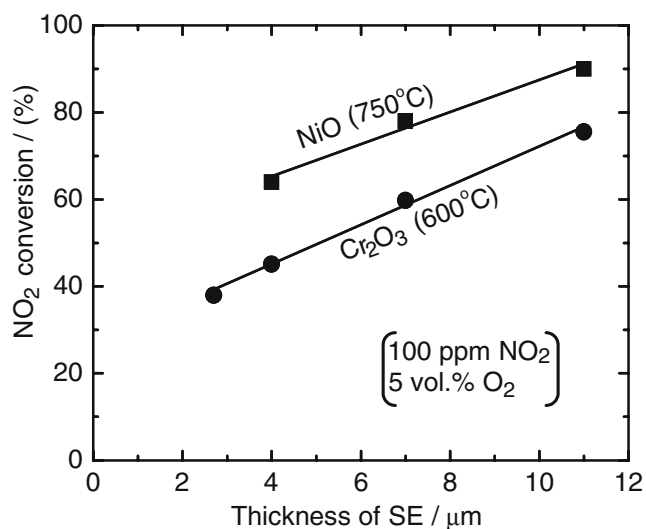
Fig. 7 Nyquist plots in the base gas and in 400 ppm NO₂ at 850 °C for the planar sensor attached with various thickness of NiO–SE under wet condition (5 vol.% H₂O)

Fig. 9 Dependence of NO_2 conversion to NO on thickness of NiO–SE (or Cr_2O_3–SE)

curve seems to be strongly depending on the thickness of SE layer.

It is seen that the cathodic polarization curve shifts upward as the thickness of SE layer is decreased and the minimum polarization current was obtained by the sensor using the thickest SE layer. This means that, because of the pronounced gas-phase NO_2 decomposition to NO through the SE layer, the NO_2 concentration at the YSZ/oxide interface can be significantly lowered when a thicker SE layer was used. As a consequence, the reaction rate (current) for the catalytic activity of cathodic reaction of NO_2 at the YSZ/oxide interface is reduced in the case of thicker SE layer. It is noted that the polarization current obtained by the sensor is the result of both electrochemical and chemical reactions occurring at the SE. Thus, the upward shift of the cathodic polarization curve with respect to decreasing thickness of SE layer can move the intersection of the cathodic and the anodic polarization curves to more positive potentials (higher sensitivity).

It is obvious that the close coincidence (ex. 58 mV [observed in Fig. 4] and 60 mV [estimated in Fig. 8], for the 7-μm-thick NiO–SE) of these intersection values in each case with that of the emf value obtained by normal potentiometric method indicates that the present sensor is based on the mixed-potential model, as has been reported before [2–8, 23–25].

Explanation of thickness effect

As mentioned above, the higher NO_2 sensitivity was obtained for the sensor using the thinner layer of SE while the lower NO_2 sensitivity was observed for the thicker SE. As the state of interface was confirmed to be same in all SE thickness (Fig. 3) and hence the rate of electrochemical

reaction, it seems that in the present case the NO_2 sensitivity is determined by the degree of the gas-phase NO_2 decomposition (see chemical equation below) occurring in the oxide–SE matrix.

$$NO_2 \rightarrow NO + 1/2O_2 \qquad (1)$$

In fact, it is reported that the gas-phase NO_2 decomposition to NO occurring in the SE matrix also plays an important role in determining the sensitivity of the mixed-potential-type sensor [2–8, 23–25]. When a thin SE is used, NO_2 can reach the YSZ/oxide interface by diffusion through the thin layer without serious decomposition of NO_2 into NO. Thus, when the sample gas containing only NO_2 is introduced to the surface of SE, the NOx composition at the YSZ/oxide interface is far from the equilibrium, i.e., NO_2 concentration is predominantly high. Such a high NO_2 concentration at the interface results in high NO_2 sensitivity. On the other hand, when the SE is rather thick, in the course of diffusion of sample gas through the thick oxide-layer, NO_2 can be easily decomposed into NO due to the pronounced gas phase reaction.

The surface of oxide grains may act as a catalyst for the NO_2 decomposition. Although NiO and Cr_2O_3 were used as a catalyst for oxidation, the gas-phase NO_2 decomposition to NO can be also catalyzed by using each of Cr_2O_3 and NiO as reported elsewhere [22, 33]. Thus, it is rather difficult for NO_2 to reach the YSZ/oxide interface without decomposition to NO in the thicker SE layer. In such a case, the NOx composition may be close to the equilibrium at the interface. As a result, the NO_2 sensitivity is lower for the device using the thicker SE. In this case, there is little driving force for the electrochemical reactions, which can reduce the mixed potential when the NOx composition comes closer to equilibrium. When the thickness of SE is in the middle, a moderate NO_2 sensitivity can be attained.

The above explanation can be verified by the results of the measurements of gas-phase NO_2 decomposition to NO occurring in the SE. So, to quantify the amount of NO_2 decomposition to NO on each of the various thicknesses of NiO (or Cr_2O_3), the gas-phase catalytic activity for the decomposition reaction (Eq. 1) was evaluated in the temperature range of 200–900 °C. Figure 9 shows the dependence of NO_2 conversion to NO on the thickness of NiO and Cr_2O_3 layers at 750 and 600 °C, respectively. It is seen that, as expected, the NO_2 conversion decreased with decreasing thickness of oxide layer and the lowest conversion is observed for the thinnest SE layer (4 μm for NiO, 2.7 μm for Cr_2O_3).

Thus, it can be said that the thickness of SE plays a very important role in deciding the sensitivity of the sensor and the higher sensitivity could be obtained by using thinner SE.

Conclusions

The mixed-potential-type sensors using YSZ plate and oxide (NiO and Cr_2O_3)–SEs having different thicknesses were fabricated and their NO_2-sensing characteristics were examined at high temperatures. It was shown that the NO_2 sensitivity was strongly dependent on the thickness of NiO–SE (or Cr_2O_3–SE) used and the highest sensitivity was obtained using each thinnest SE layer. It was observed that the response/recovery rates were almost equal irrespective of the thickness of SEs. Based on the results obtained from the measurements of complex impedances, polarization curves, and gas-phase catalysis, it was speculated that the NO_2 sensitivity in the present case is mainly controlled by the degree of gas-phase decomposition of NO_2 to NO occurring on the surface of oxide–SE.

References

1. Traversa E (1995) J Am Ceram Soc 78:2625
2. Miura N, Kurosawa H, Hasei M, Lu G, Yamazoe N (1996) Solid State Ionics 86–88:1069
3. Miura N, Lu G, Yamazoe N (1998) Sens Actuators B 52:169
4. Lu G, Miura N, Yamazoe N (1998) Ionics 4:16
5. Miura N, Lu G, Yamazoe N (2000) Solid State Ionics 136–137:533
6. Bartolomeo ED, Traversa E, Baroncini M, Kotzeva V, Kumar RV (2000) J Eur Ceramic Soc 20:2691
7. Geopel W, Reinhardt G, Rosch M (2000) Solid State Ionics 136–137:519
8. Ono T, Hasei M, Kunimoto A, Yamamoto T, Noda A (2001) JSAE Rev 22:49
9. Zhuiykov S, Muta M, Nakano T, Hasei M, Yamazoe N, Miura N (2001) Electrochem Solid State Lett 4:H19
10. Yoon JW, Grilli ML, Bartolomeo ED, Polini R, Traversa E (2002) Sens Actuators B 76:483
11. Miura N, Zhuiykov S, Ono T, Hasei M, Yamazoe N (2002) Sens Actuators B 83:222
12. Zhuiykov S, Ono T, Yamazoe N, Miura N (2002) Solid State Ionics 152–153:810
13. Szabo NF, Du H, Akbar SA, Soliman A, Dutta PK (2002) Sens Actuators B 82:142
14. Mukundan R, Brosha EL, Garson FH (2003) J Electrochem Soc 150:H279
15. Skelton DC, Tobin RG, Lambert DK, DiMaggio CL, Fisher GB (2003) Sens Actuators B 96:46
16. Ono T, Hasei M, Kunimoto A, Miura N (2003) Electrochemistry 71:405
17. Ono T, Hasei M, Kunimoto A, Miura N (2004) Solid State Ionics 175:503
18. Miura N, Akisada K, Wang J, Zhuiykov S, Ono T (2004) Ionics 10:1
19. Zhang W-F, Schmidt-Zhang P, Guth U (2004) Solid State Ionics 169:121
20. Miura N, Wang J, Nakatou M, Elumalai P, Zhuiykov S, Terada D (2005) Ceram Eng Sci Proc 26:3
21. Elumalai P, Wang J, Zhuiykov S, Terada D, Hasei M, Miura N (2005) J Electrochem Soc 152:H95
22. Miura N, Wang J, Nakatou M, Elumalai P, Hasei M (2005) Electrochem Solid State Lett 8:H9
23. Elumalai P, Miura N (2005) Solid State Ionics 176:2517
24. Miura N, Wang J, Nakatou M, Elumalai P, Zhuiykov S, Hasei M (2005) Sens Actuators B 114:903
25. Wang J, Elumalai P, Terada D, Hasei M, Miura N (2006) Solid State Ionics 177:2305
26. Martin LP, Quoc Pham A, Glass RS (2005) Sens Actuators B 96:53
27. Elumalai P, Hasei M, Miura N (2006) Electrochemistry 74:197
28. Kunimoto A, Hasei M, Yan Y, Gao Y, Ono T, Nakanouchi Y (1999) SAE Tech Pap Ser 1999-01-1280
29. Hyodo T, Mori T, Kawahara A, Katsuki H, Shimizu Y, Egashira M (2001) Sens Actuators B 77:41
30. Miura N, Nakatou M, Zhuiykov S (2003) Sens Actuators B 93:221
31. Elumalai P, Miura N (2004) In: Bruckner-Lea S, Vanýsek P, Hunter G, Mukundan R, Miura N, Mizutani F (eds) Chemical sensors VI: chemical and biological sensors and analytical methods. Proceedings of the Electrochemical Society, vol 2004-08. Pennington, NJ, pp 80–88
32. Nakatou M, Miura N (2004) Electrochem Commun 6:995
33. Szabo NF, Dutta PK (2004) Solid State Ionics 171:183